LOAN DOCUMENT

PHOTOGRAPH THIS SHEET

DTIC ACCESSION NUMBER

LEVEL

INVENTORY

Analysis of Radiometer Data from the Vol 9 SA-2 Static Firing

DOCUMENT IDENTIFICATION

2000

DISTRIBUTION STATEMENT A
Approved for Public Release
Distribution Unlimited

DISTRIBUTION STATEMENT

HANDLE WITH CARE

ACCESSION FOR
NTIS GRA&I ☑
DTIC TRAC ☐
UNANNOUNCED ☐
JUSTIFICATION

BY

DISTRIBUTION/

AVAILABILITY CODES

DISTRIBUTION	AVAILABILITY AND/OR SPECIAL	
A-1		

DISTRIBUTION STAMP

DATE ACCESSIONED

DATE RETURNED

20000814 217

DATE RECEIVED IN DTIC

REGISTERED OR CERTIFIED NUMBER

PHOTOGRAPH THIS SHEET AND RETURN TO DTIC-FDAC

DTIC FORM 70A JUN 90

DOCUMENT PROCESSING SHEET

PREVIOUS EDITIONS MAY BE USED UNTIL STOCK IS EXHAUSTED.

LOAN DOCUMENT

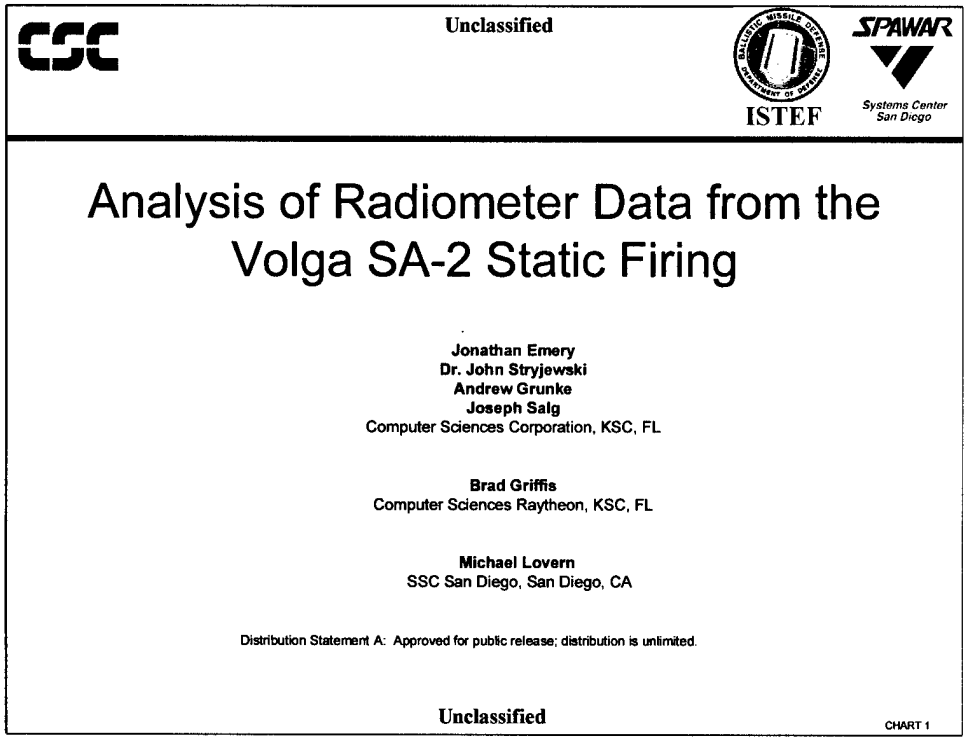

Abstract

The Ballistic Missile Defense Organization's (BMDO) Innovative Science and Technology Experimentation Facility (ISTEF[1]) collected data from the test stand firing of a Volga (SA-2 Mod 3 5Я23) engine. The test was conducted at the Redstone Technical Test Center (RTTC) Test Area 5 on September 15, 1999. Signatures were measured using a non-imaging radiometer and a suite of imaging instruments ranging from the ultraviolet through long wave infrared, as well as laser backscatter and transmission measurements. This paper reports the results of the measurements made with the radiometer. The objectives of the radiometer experiment were to show that the signal from the plume could be detected and that useful information could be extracted. The AC component of the total plume intensity was separated from the large DC component and recorded with a high gain AC-coupled silicon detector. Standard Fourier techniques were used to recover the Power Spectral Density (PSD). By examination, the largest spectral component of the PSD was related to the turbo-pump frequency. Further filtering techniques provided excellent gains in the signal to noise ratio. The radiometer has since been used to collect data on Atlas II vehicles during boost and has repeated the ability to detect turbo-pump frequencies at ranges exceeding 10 km. Ongoing efforts include demonstration of the ability to measure combustion chamber acoustical modes[2], which may yield critical engine performance information such as thrust and chamber dimensions. This will lead to a more complete understanding of the mechanism that allows measurement of the relatively low pump frequencies. These measurements point out the ability to measure and process information that may prove useful for booster typing and target identification for Boost Phase Intercept (BPI) programs such as ABL and SBL.

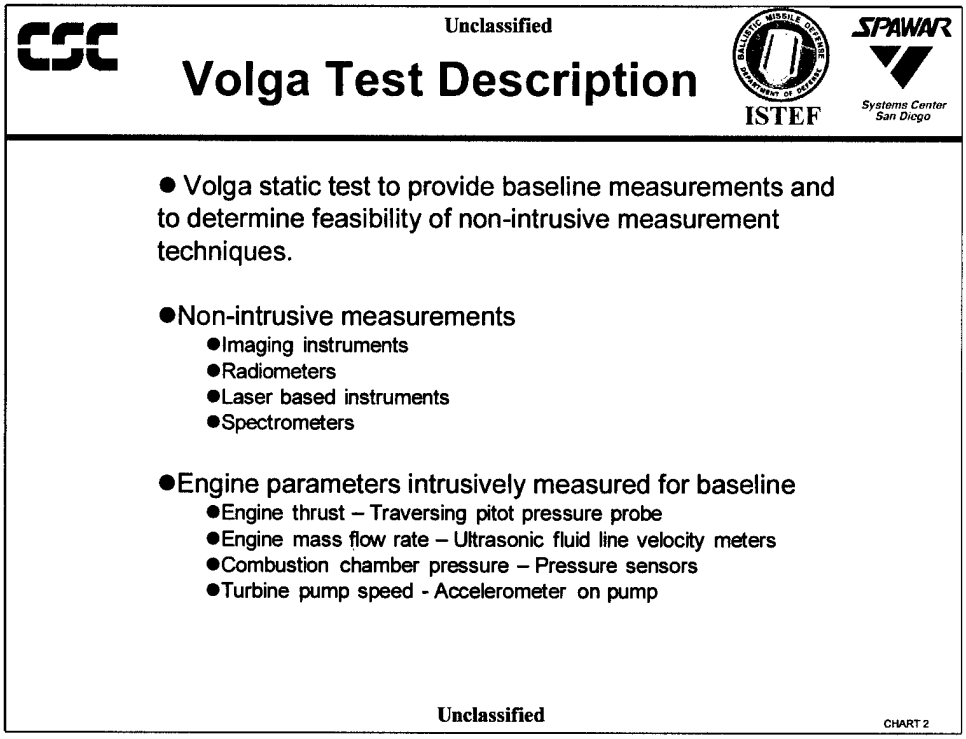

Volga Test Description

The static test[3] of the SA-2 Mod 3 5Я23 engine at the RTTC took place on September 15, 1999 at Test Area 5. The 55 second test was conducted for the purpose of establishing the propulsion system baseline performance and to discover the feasibility of non-intrusive determination of critical engine performance parameters. Native propellants IRFNA and TONKA* were used. The engine was placed in the vertical test stand with approximately 3m of space between the engine nozzle exit and the entrance to the flame bucket. The non-intrusive instrumentation included imaging instruments, spectrometers, radiometers and laser based instruments. In addition to the non-intrusive measurements, more direct measurements were made to provide baseline data. Engine thrust was inferred by a traversing pitot pressure probe on a ram. The pressure probe was deployed and retracted twice during the test, giving a pressure profile in the horizontal plane a known distance from the nozzle. The engine mass flow rate was measured by strap-on ultrasonic oxidizer and fuel fluid line velocity meters. Combustion chamber pressure was determined by pressure sensors in the combustion chamber. Turbine pump speed was measured by an accelerometer on the turbo-pump. The ISTEF radiometer was deployed as an instrument to non-intrusively measure the turbine pump frequency. The effectiveness of the radiometer to measure this parameter and potential for other measurements is the focus of this paper.

* IRFNA- Inhibited Red Fuming Nitric Acid. TONKA-50% Triethyl Amine, 50% Xylidene

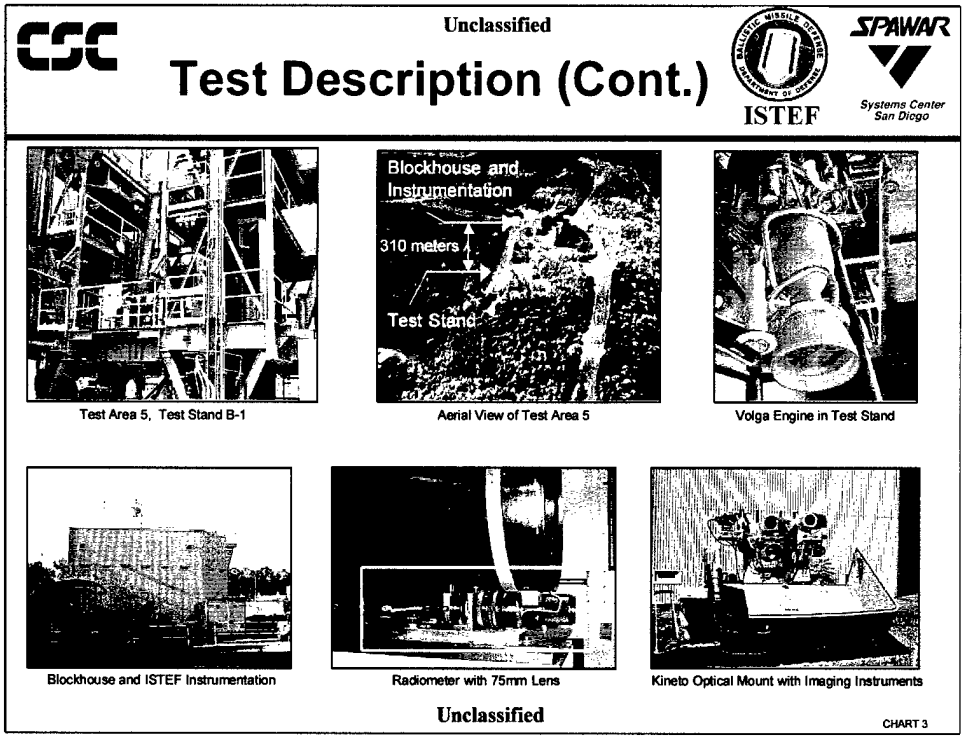

Test Description (continued)

The ISTEF equipment was positioned approximately 310 meters from the test stand adjacent to the block house. A trailer housed the active instrumentation and the radiometer. The imaging instruments were installed on a Kineto optical tracking mount and operated from a separate control trailer. The Volga engine is shown installed in the test stand. The turbo-pump exhaust outlet is visible just to the left of the nozzle.

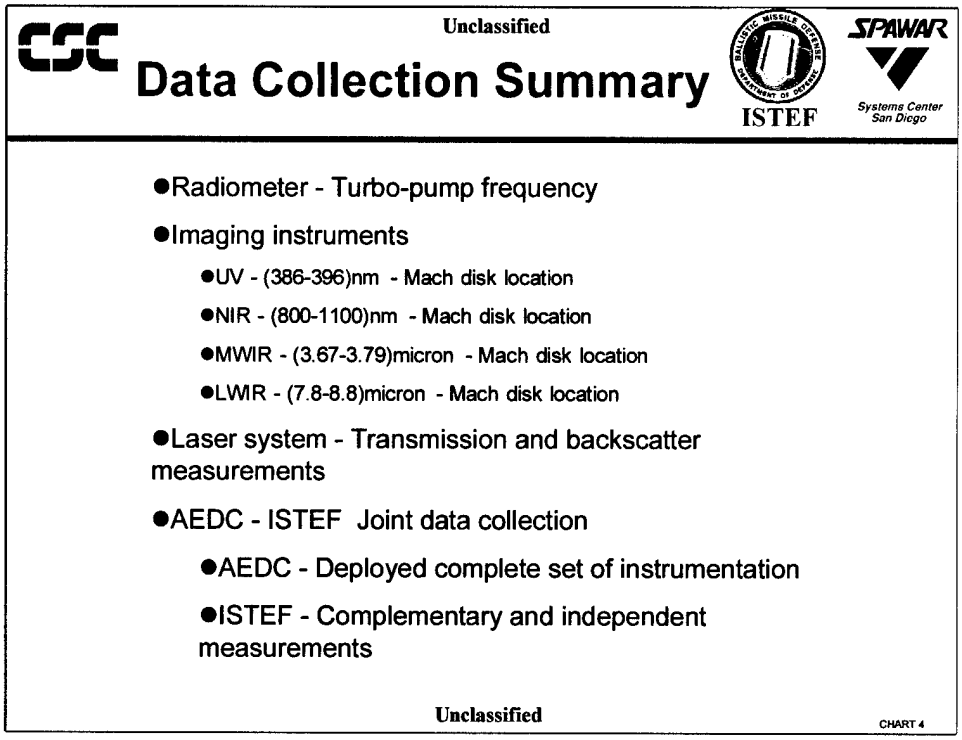

Data Collection Summary

In addition to the radiometer data that is discussed in this report, a description of the other ISTEF systems that collected data for the Volga test is warranted. Four calibrated imaging instruments were used:

Sensor	Optic	Wavelength	Vertical FOV	
			(mrad)	meters at target
UV Xybion/Hamamatsu	Celestron	386-396 nm	12.0	4.1
NIR Panasonic 400	Zoomar	0.80 - 1.1 nm	9.1	3.0
MWIR Amber InSb 4256	ISTEF SFP	3.67 - 3.79 microns	10.9	3.7
LWIR JPL QWIP/4256	ISTEF SFP	7.8-8.8 microns	10.9	3.7

Each of the imaging instruments was able to identify the mach disk location. The shorter wavelength UV and NIR instruments detected more of the surface effects of the plume and observed pronounced shockwaves including a double mach disk at the first mach disk location. The longer wavelength MWIR and LWIR instruments detected more of the core features of the plume and less defined mach disks (mach diamonds were more visible than in the MWIR/LWIR than in the UV and NIR). The laser system measured the plume transmission and backscatter at two laser wavelengths, 532nm and 1064nm. These are the fundamental and frequency doubled wavelengths of Nd:YAG. The results show significantly more transmission than was anticipated indicating less soot content than predicted. The backscatter results indicate possible evidence of fuel droplets in the plume.

The AEDC (Arnold Engineering Development Center) deployed a complete set of instruments consisting of imaging systems, radiometers, spectrometers and laser based systems. ISTEF's participation provided complementary and independent measurements for the Volga test.

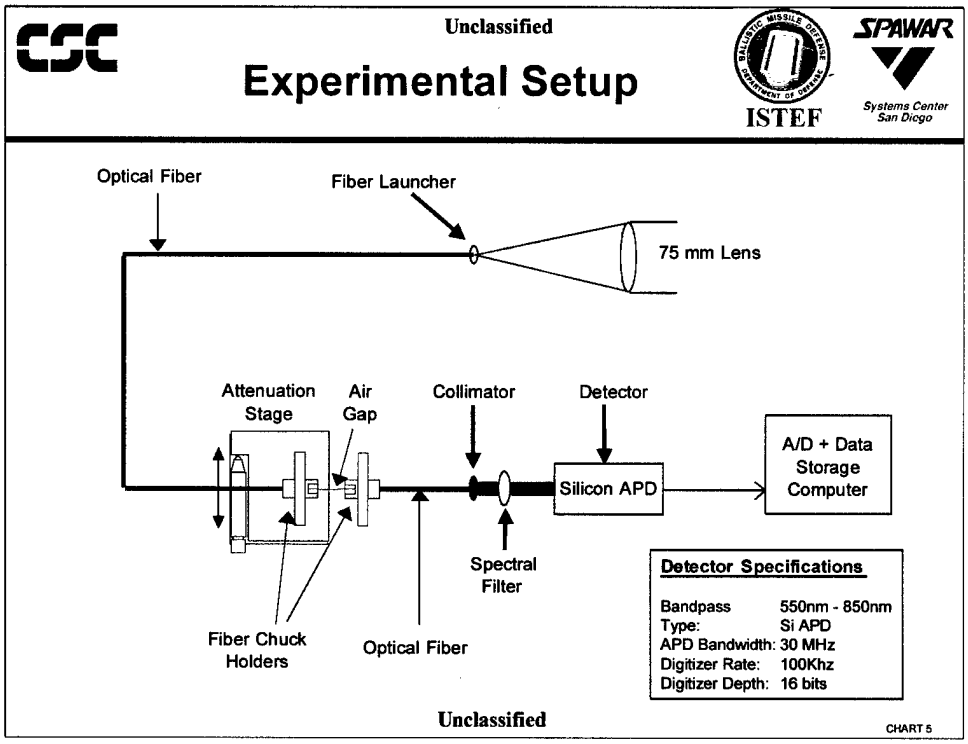

Experimental Setup

The signal path of the radiometer originates at the lens. The light bundle is focused directly into the fiber. The fiber is routed to the optical attenuator which has two fiber chuck holders and an air gap between them. One chuck holds the fiber stationary while the other may translate normal to the direction of light propagation. The degree of attenuation is directly related to the area of overlap between the two circular apertures. The output of the fiber is collimated by a microscope objective. The light passes through a spectral filter and onto the detector. The detector, a silicon avalanche photodiode (APD), converts the optical signal to an analog electrical signal where an A/D stage converts the analog signal to digital and the data are recorded using a PC. The digitizer accepts 0 to 10 volts at 16 bits of resolution. The field of view of the instrument is determined by the focal length of the collector and the diameter of the fiber where:

$$FOV = l_d / fl \quad (l_d = \text{diameter of fiber, } fl = \text{focal length of collector}) \qquad (1)$$

A 75mm (f/1.4) lens was used for the light collector. The fiber was 400 micron multi-mode silica glass, step index fiber. This yielded a field of view of 5.3 mrad. The sensor was positioned approximately 310 meters from the test stand giving a spot size at the target of 1.65 meters. A pulsed (30 Hz) Nd:YAG laser illuminating a target board was used to align the radiometer to the desired position. The top of the field of view was aligned just above the nozzle of the engine. During the test, the Nd:Yag laser was operating at 532nm and 1064nm for collection of transmission and backscatter data except during a 5 second laser shutdown period from 25 to 30 seconds TAI (Time After Ignition). Spectral filters were used to inhibit laser induced response from the radiometer forming an optical passband of 550nm to 850nm.

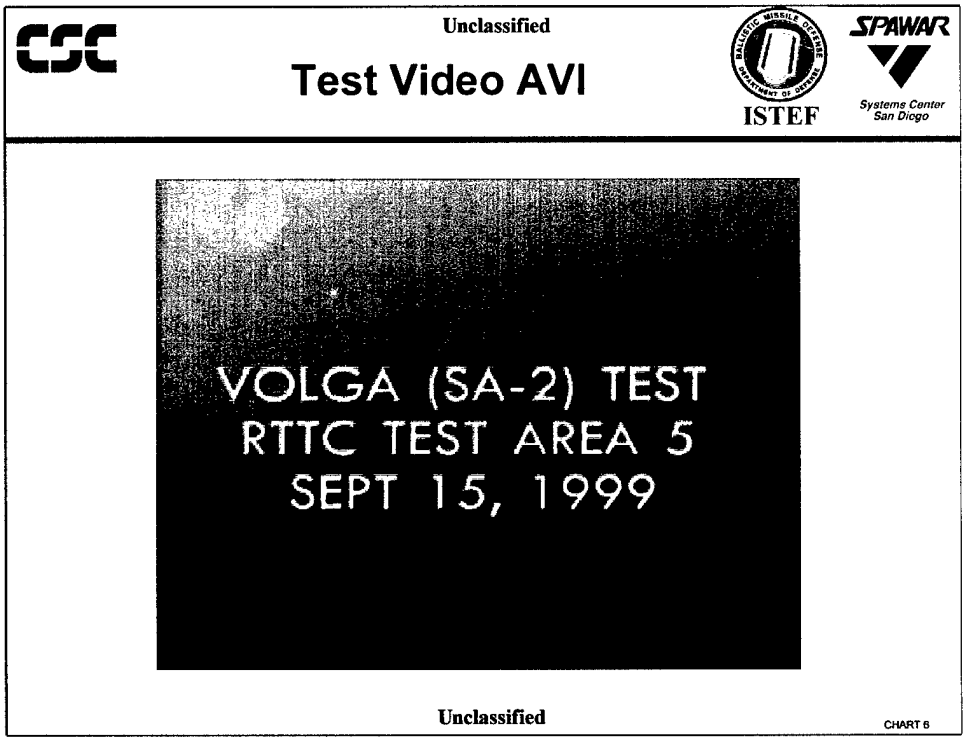

Test Video AVI

Shown here is a video sequence of the Volga test. The full screen view is from a documentary visible/NIR camera with a vertical field of view of 1.18 mrad. The inlay at the upper left of the video is from the calibrated NIR system with a vertical field of view of 9.1 mrad. Ignition is observed at the beginning of the sequence with the engine reaching steady state within about 1 second. The double mach disk is visible in the inlay. Note the disturbance in the plume as the pressure probe traverses the plume. Shutdown occurs at ~54 seconds TAI followed by exhaustion of the propellants as the engine surges for about 15 seconds.

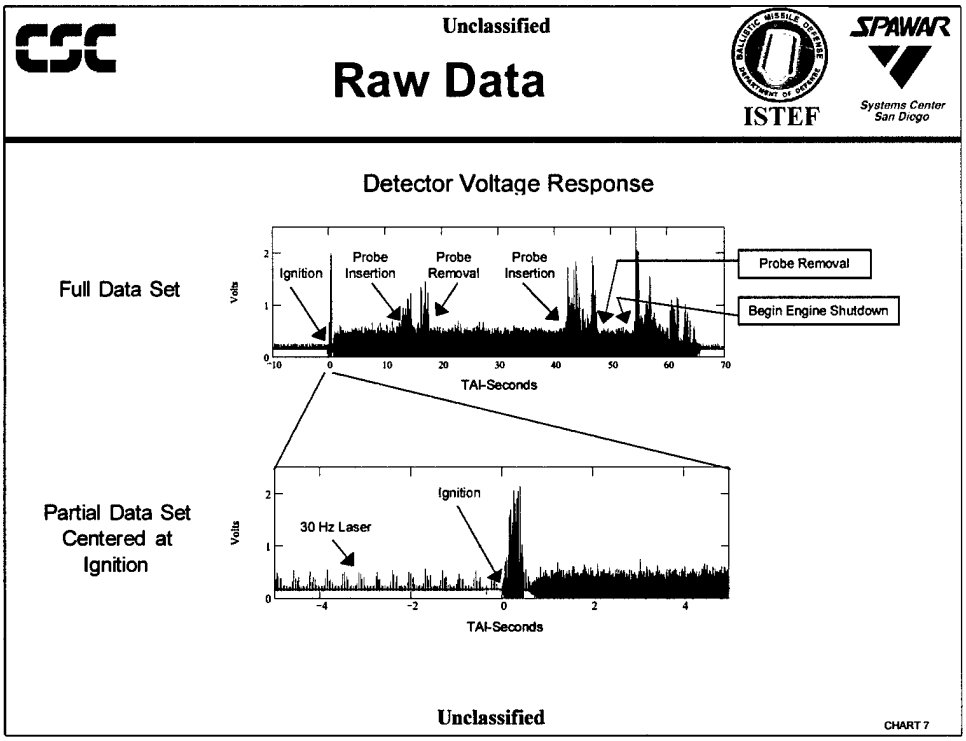

Raw Data

Data were successfully recorded from engine ignition through engine shutdown. Several events appear in the raw data. Before ignition, the 30 Hz pulse train from the laser is apparent. At ignition, a large transient is clearly visible before the engine settles into steady state (with respect to the radiometer) at about 1 second TAI. The pressure probe insertions and removals also are visible as increases in signal level and transients. Engine shutdown was marked by a sudden drop in signal level and then the appearance of several large transients over about a 15 second period as the engine exhausted the remaining propellants.

The voltage did not exceed 2.5 volts and no attenuation was required during the test After ignition, it appears that the lower portion of the signal has been clipped. Since the digitizer was configured to record 0 to 10 volts, any response below 0 volts was clipped resulting in a 1-2 dB loss in SNR. Any spectral artifacts from this truncation would be related to the 100kHz sampling rate and no artifacts in the 0 to 5 kHz range have been found. For future data collections, the digitizer will be configured to also record negative voltages.

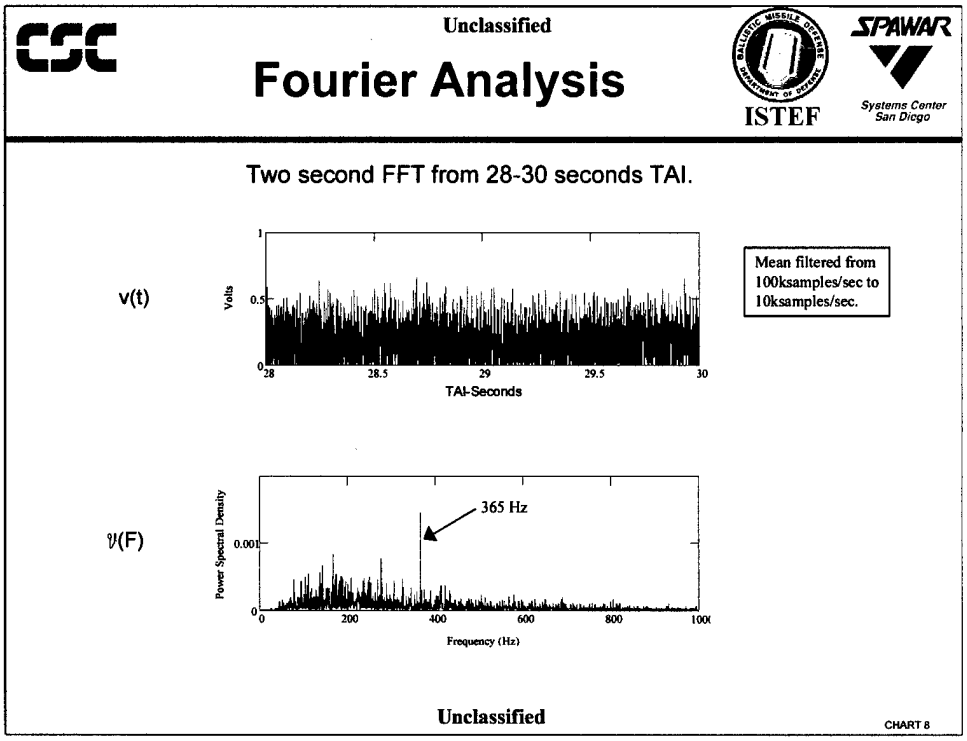

Fourier Analysis

Several segments of the test were initially analyzed for spectral content at the full 100kHz sample rate. The large quantity of data was unwieldy and the original 100kHz data was mean filtered to 10kHz. To insure the sub-sampling technique did not introduce artifacts into the frequency region of interest of less than 5kHz, several sequences from both sampling rates were compared in frequency content. There was no apparent information loss or introduced artifacts in the frequency range of less than 5kHz. A two second time domain segment example is shown with the corresponding frequency domain. It was produced with a standard FFT routine with a square window. A large frequency component at 365 Hz is noted. The general spectral shape or continuum is similar throughout the test with a rise from the floor at about 50 Hz, a peak at just below 200 Hz and a decline with increasing frequency to the noise floor. Near the 200 Hz region, there are large fluctuations in amplitude of individually occurring frequency components but the bell shaped envelope remains. This may be a characteristic of this particular combustion chamber[2].

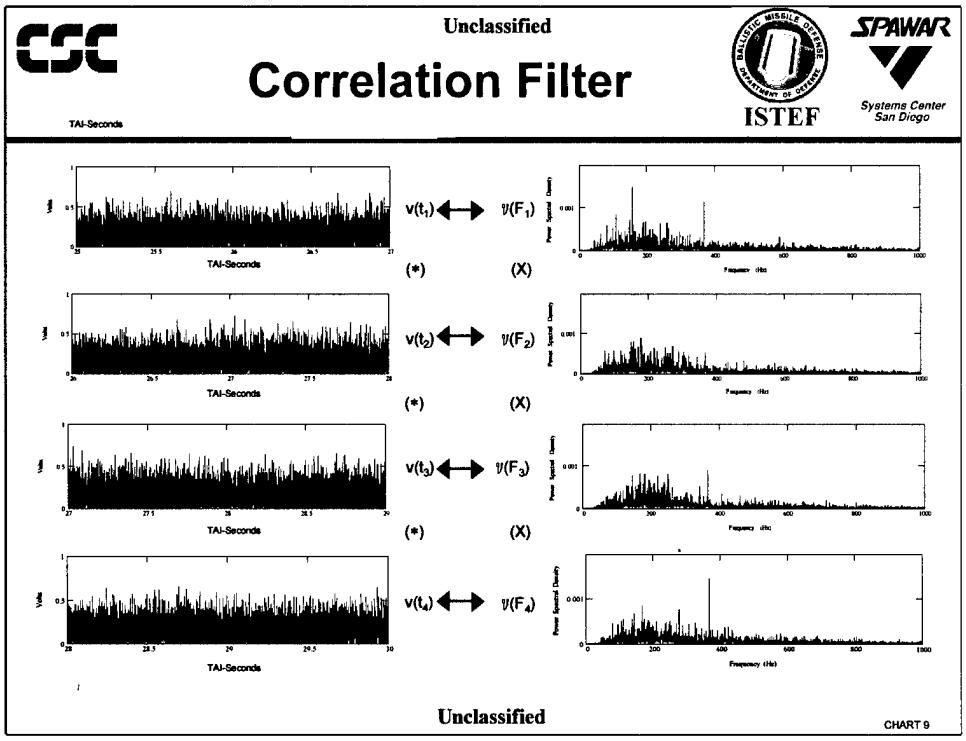

Correlation Filter

To distinguish transient events from steady state events, a correlation filter was used (Although transient events are not treated in this paper, they may be important in their own right in determining performance measures[2]). The example shown here is restricted to the 5 second laser shutdown period to insure there is no spectral contamination from the laser. Four two-second segments with a one-second overlap were analyzed. The corresponding Fourier transform was calculated for each. The four frequency domain segments were multiplied with respect to frequency:

$$V_{corr}(F) = V(F_1) \times V(F_2) \times V(F_3) \times V(F_4) \qquad (2)$$

Those spectral components that are driven by steady state events tend to be more constant. Transient events are, by definition, not constant and should take on small values at least periodically. The multiplying process therefore causes the transient events to be reduced in magnitude while leaving the steady state components largely unchanged. There are some tradeoffs to be aware of in determining the time interval chosen for each segment and the number of segments chosen to process. As the time interval increases, there could be actual temporal changes in the steady state frequency components which would cause unintentional suppression of the steady state frequency components. As the time interval decreases, the transient events tend to have a higher spectral contribution with respect to the steady state contributions. The minimum time interval is established by the Nyquist rate:

$$T_{min} = \frac{1}{2 f_{max}} \qquad (3)$$

where f_{max} is the maximum frequency expected to be measured.

Unclassified

Correlation Filter Results

ISTEF

SPAWAR Systems Center San Diego

Four Frame Correlation Filter

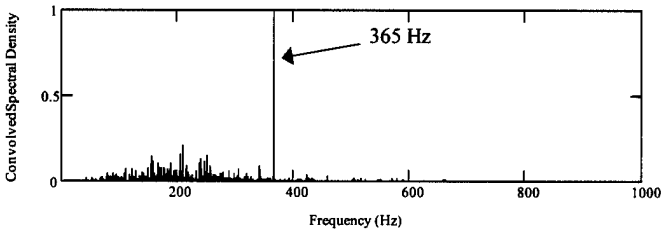

- Turbo-pump frequency confirmed at 365 Hz
- No other large steady state frequencies present

Unclassified

CHART 10

A similar tradeoff is associated with the number of segments to include in the correlation filter. As the number of segments increases, actual temporal changes in the resonant frequency may lead to suppression of steady state frequency components. As the number of segments decreases, the transient events may not be suppressed enough to distinguish them from steady state events. In a real-time application, the minimum time interval and minimum number of segments would be the goal to minimize processing time.

In the four frame correlation filter example, the component at 365 Hz has reached a signal to continuum ratio of ~ 4:1. The characteristic bell shape is still present although reduced relative to the 365 Hz component. The 365 Hz component has been confirmed as the turbo-pump frequency from reduction of the data from the accelerometer mounted on the turbo-pump.

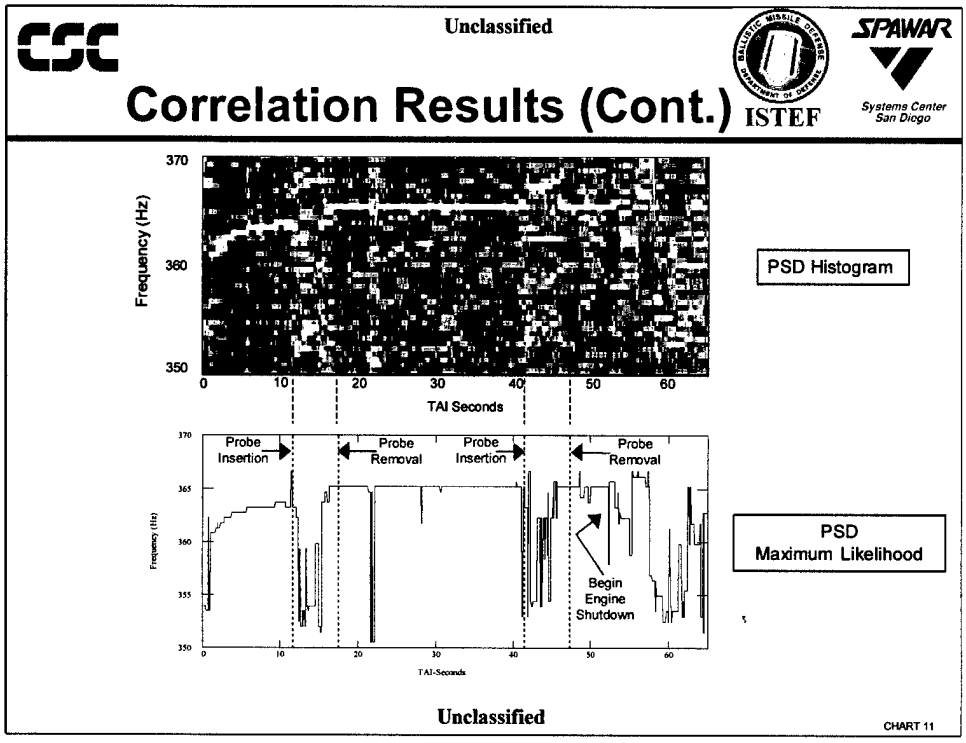

Correlation Results (Cont.)

Shown above is a PSD histogram that spans the full test. Each column represents results from a two-second width sliding window FFT with a 0.1 second $\Delta\tau$ between columns. Lighter or whiter pixels indicate greater corresponding power in that spectral bin. The PSD Maximum Likelihood chart plots the largest power frequency value for that temporal bin in the PSD Histogram. A transient is seen at ignition followed by a ramp up in frequency. Fluctuations can be seen as the pressure probe interfaces with the plume. Engine shutdown is followed by a period of transient activity. The most stable period appears between the two probe interface times, but this period also has transient activity.

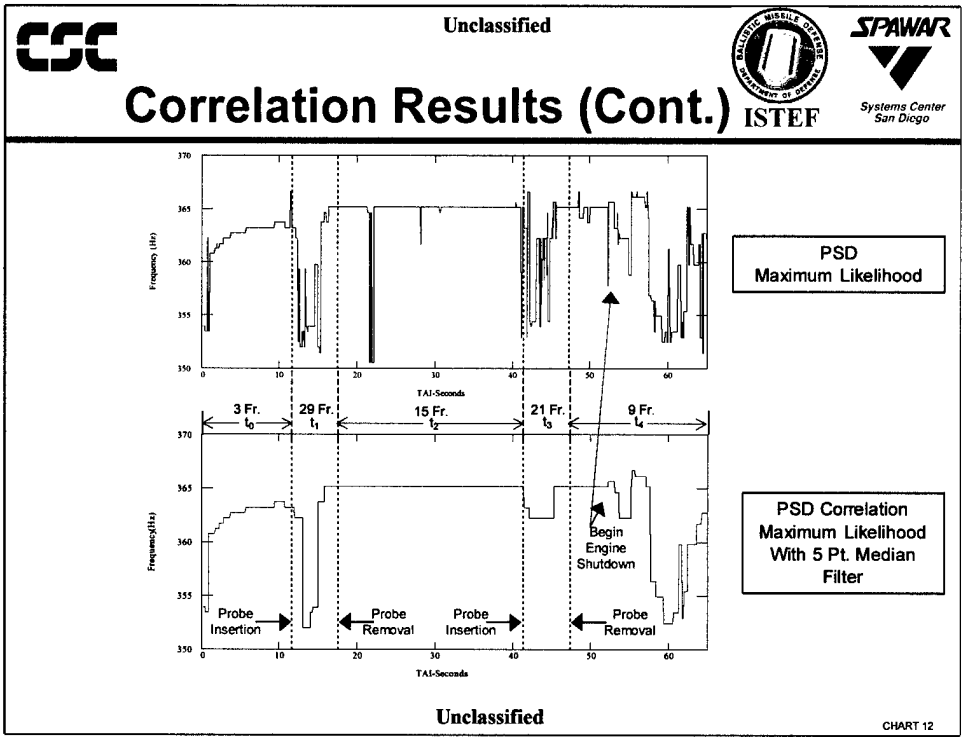

Correlation Results (Cont.)

The PSD Maximum Likelihood chart is shown again here for comparison purposes. Also shown is the correlation filter applied to the time series FFT. Five temporal periods have been identified that have been manually optimized for the number of frames to include in the correlation filter. A 5 pt. median filter is then applied to the maximum likelihood frequency and plotted. This filter implementation performs well under steady state conditions and easily yields the turbo-pump shaft frequency. During periods of transient activity as in engine ignition or shutdown, the filter is not well behaved.

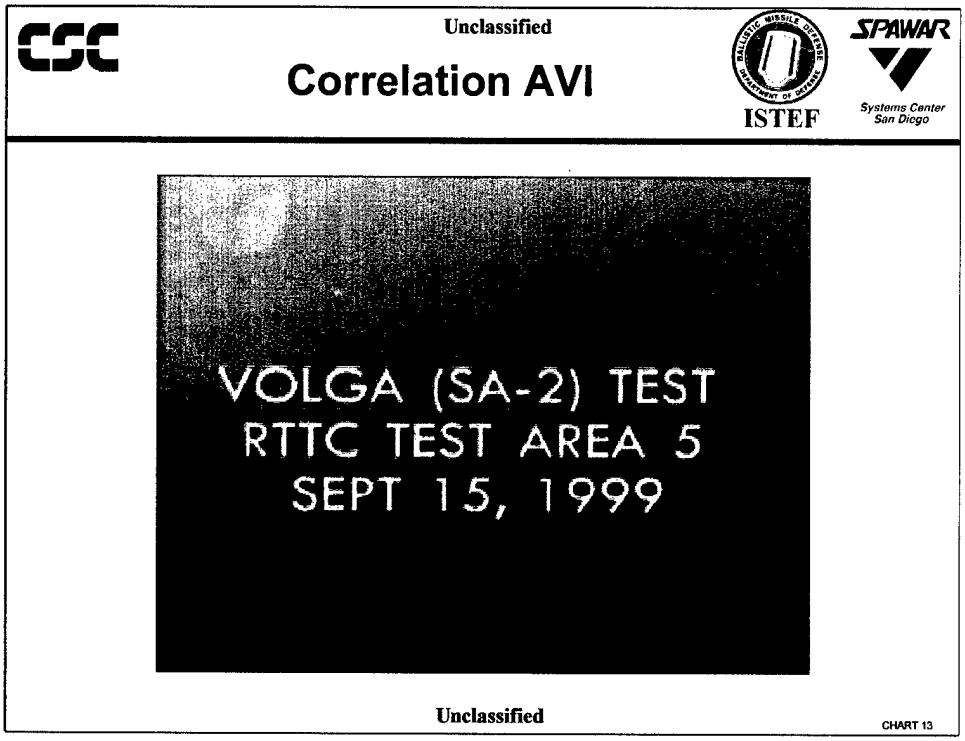

Test Video AVI

Shown here is a video sequence of the Volga test. The full screen view is from a documentary Visible-NIR camera with a vertical field of view of 1.18 mrad. The inlay at the upper left of the video is from the calibrated NIR system with a vertical field of view of 9.1 mrad. A second inlay at the lower left contains the results of the correlation filter, shown in red, with amplitude on the y-axis and frequency on the x-axis. Also plotted in black are raw unfiltered points from the FFT routine for comparison purposes.

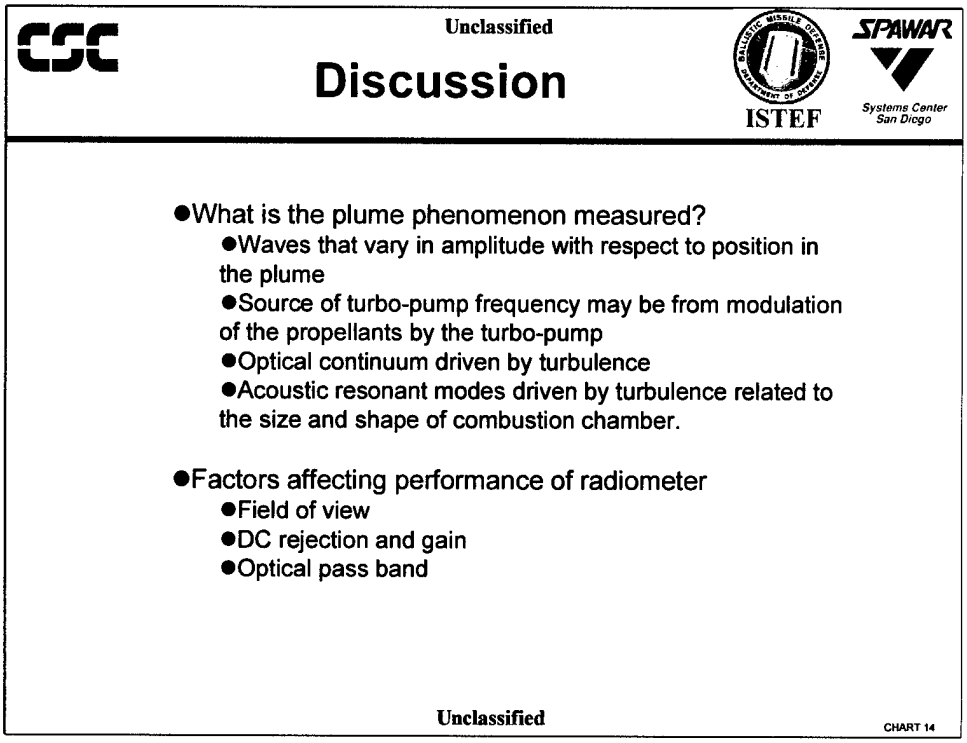

Discussion

Understanding the mechanism that enables measurement of the optical fluctuations in the plume allows us to evaluate several factors that affect the performance of the radiometer. The plume can be thought of as a composite of optical waves that vary in amplitude with respect to position in a reference frame moving with the same velocity vector as the plume or with respect to time in the reference frame of the engine normal to the plume velocity. Modulation of the propellants by the turbo-pump is a possible source of the optical waves related to the shaft frequency, although no harmonics related to the blade count of the turbine, oxidizer pump or fuel pump have been found in the radiometer data. Turbulence in the combustion chamber and nozzle also cause optical waves and form a continuum. Previous measurements reveal longitudinal and transverse resonant modes[2] that can be related to the size and shape of the combustion chamber and nozzle. These "acoustic" resonances are thought to be driven by turbulence in the nozzle and are superimposed upon the continuum. The measurements were made in the NIR/MWIR range and no evidence of these resonances have been found in the Volga radiometer data.

The field of view of the instrument plays an important role in the range of frequencies that can be measured by the instrument. As the wavelength λ increases beyond half of the field of view, the ability to detect that wave is diminished due to averaging where:

$$\lambda = \frac{Velocity_{plume}}{Frequency} \qquad (4)$$

When λ is modulo the field of view, it should result in complete cancellation of that wave. Selection of too large of a field of view has a band limiting effect on measurements. Another factor to consider is the choice of detector. Since a large DC component is coupled with the AC component of the plume, a suitable detector should be capable of rejecting the DC component while still having enough bandwidth and gain to measure the AC component. The optical pass-band of the detector must also be within the spectral range that the optical phenomenon occurs.

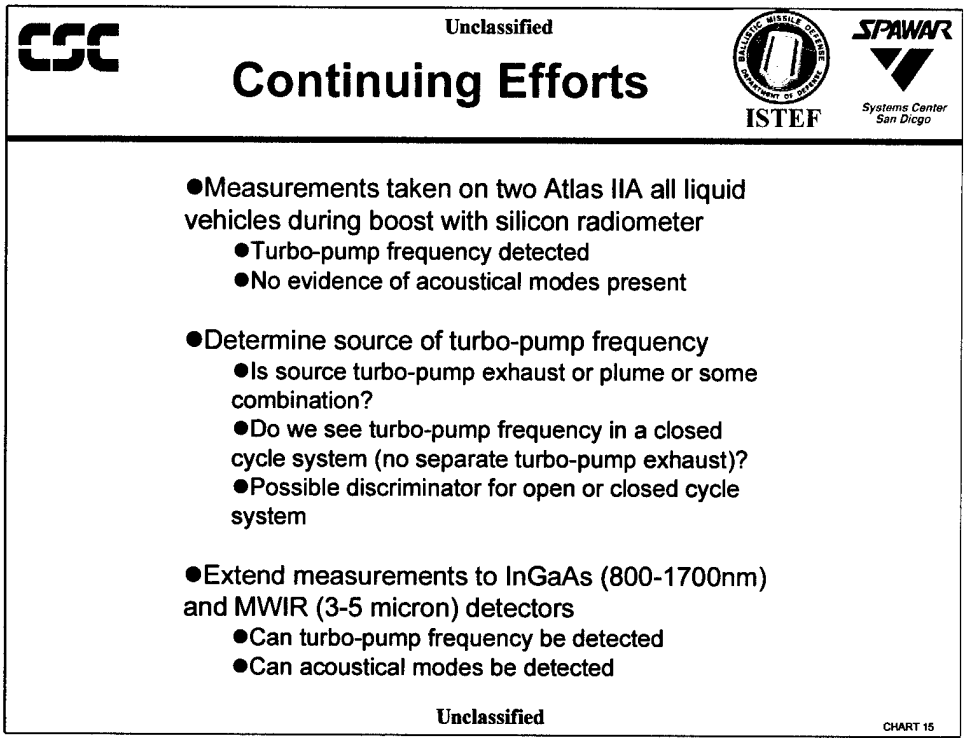

Continuing Efforts

Determining the source of the turbo-pump frequencies is of great interest. ISTEF has observed two Atlas IIA vehicles during boost from the Eastern Range and has detected frequency components corresponding to the turbo-pump. However, preliminary examination of data acquired from the new Atlas III vehicle did not reveal an obvious frequency component that could be related to the turbo-pump. One design difference that may explain this is that the Atlas III employs closed cycle engine technology where the turbo-pump exhaust is routed through the combustion chamber instead of exhausting directly to the atmosphere. This could mask the turbo-pump frequencies. Further attempts to measure the acoustical modes in rocket plumes could be rewarding since literature[2] shows that the information contained in these modes can provide critical details about the booster design and operation. Extension of data collection bands into the near infrared with InGaAs detectors and the mid-wave infrared with InSb or HgCdTe detectors and optimization of the instrument field of view may facilitate measurement of the acoustical modes.

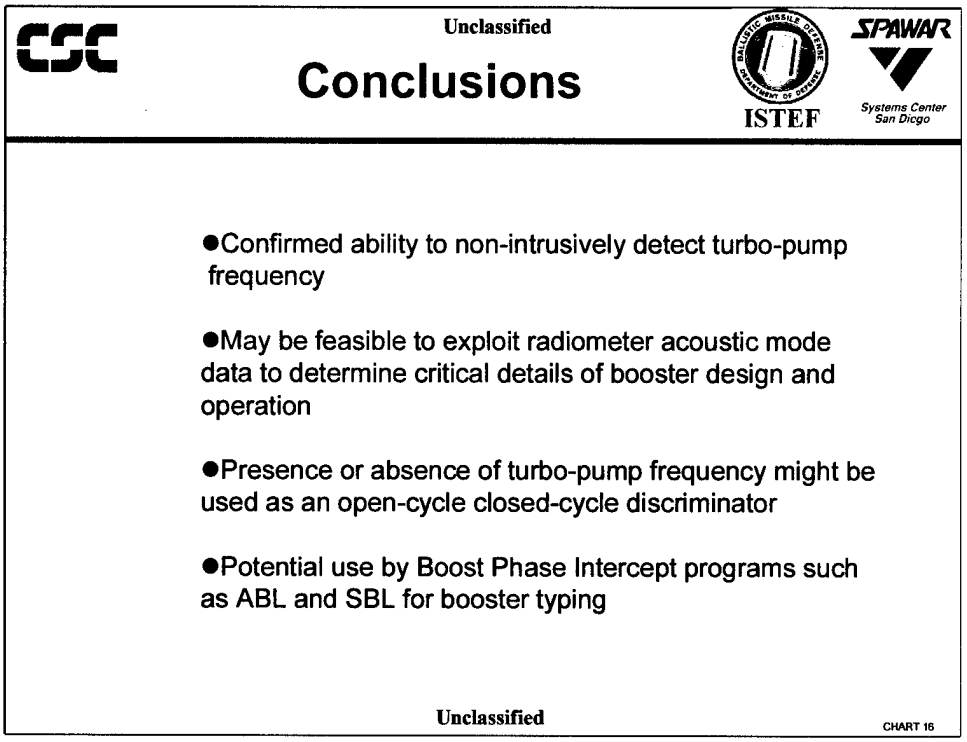

Conclusions

The Volga test results show that the turbo-pump rotation rate can be detected non-intrusively. This is significant since the shaft rotation rate is a natural booster typing signature. The presence or absence of the turbo-pump frequencies also may indicate whether the booster is open or closed cycle. It may further be possible to extract other critical details of booster design and operation by detecting the acoustic modes. The data suggest that it may be possible to incorporate a radiometer based instrument to augment the existing booster typing capability providing a significant capability for boost phase interceptor programs such as ABL and SBL.

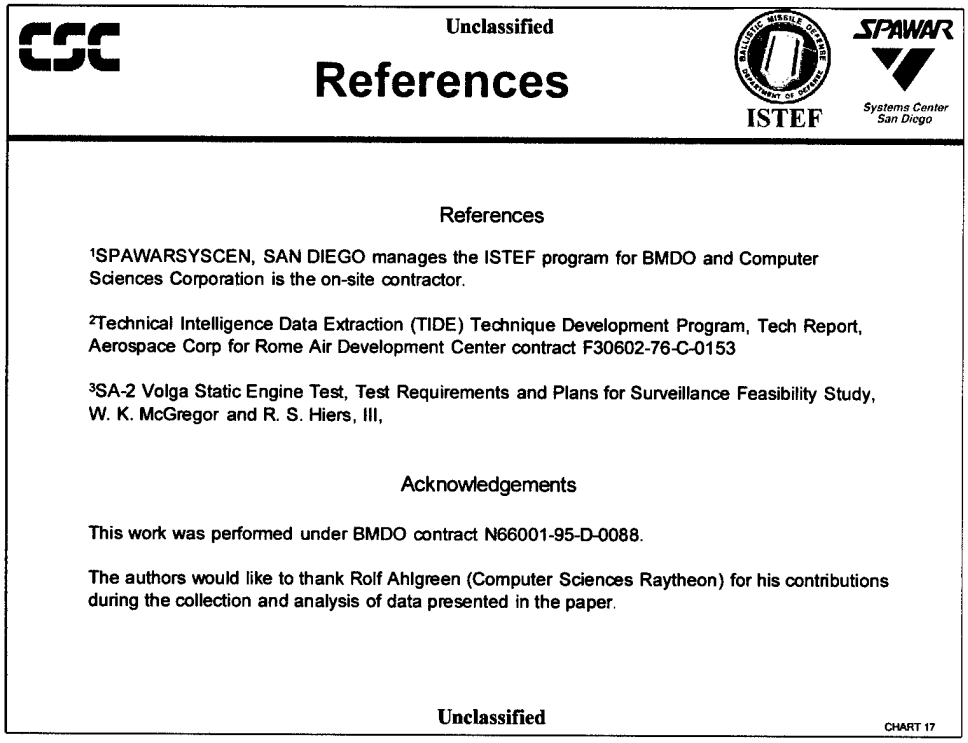

References

[1]SPAWARSYSCEN, SAN DIEGO manages the ISTEF program for BMDO and Computer Sciences Corporation is the on-site contractor.

[2]Technical Intelligence Data Extraction (TIDE) Technique Development Program, Tech Report, Aerospace Corp for Rome Air Development Center contract F30602-76-C-0153

[3]SA-2 Volga Static Engine Test, Test Requirements and Plans for Surveillance Feasibility Study, W. K. McGregor and R. S. Hiers, III,

Acknowledgements

This work was performed under BMDO contract N66001-95-D-0088.

The authors would like to thank Rolf Ahlgreen (Computer Sciences Raytheon) for his contributions during the collection and analysis of data presented in the paper.